Full Length Research Paper

Substrate molecule enhances the thermostability of a mutant of a family 11 xylanase from *Neocallimastix patriciarum*

Chun You, Hanying Yuan, Qiang Huang* and Hong Lu*

State Key Laboratory of Genetic Engineering, School of Life Sciences, Fudan University, 220 Handan Road, Shanghai 200433, China.

Thermophilic xylanases are ideal for many industrial processes operated at elevated temperatures. Here, we report a mutant of a family 11 xylanase (Xyn-CDBFV) from *Neocallimastix patriciarum* with a mutation (D57N) in the active center could be further stabilized by the substrate. Despite that the thermostability of the two enzymes are almost the same in the absence of the substrate, the mutant displays a 10 - 15°C higher optimal temperature of activity than the wild type. Potential hydrogen bonding interactions predicted by molecular docking between the substrate molecule and residues N57, E202 of the mutant are probably responsible for the stabilizing effect. This suggests that it will be useful to consider the stabilizing effect induced by the substrate in optimization processes of enzyme thermostability.

Key words: Xylanase, substrate, enzyme activity, thermostability, protein engineering, molecular docking.

INTRODUCTION

Industrial processes such as paper bleaching are usually operated at elevated temperatures. Thus, ideal industrial enzymes such as xylanase should be highly active at high temperatures. So, it is very interesting to engineer thermophilic xylanases, which have been created from mesophilic enzymes by site-directed mutagenesis and directed evolution (Dumon et al., 2008; Jeong et al., 2007; Miyazaki et al., 2006; Ruller et al., 2008; Stephens et al., 2007). In general, the thermal stabilizing effect on these mutant xylanases can be attributed to various intrinsically structural features, such as more surface charged residues (Turunen et al., 2002), disulfide bridge (Fenel et al., 2004; Wakarchuk et al., 1994b; Xiong et al., 2004; Yang et al., 2007) and higher degree of hydrophobic packing in protein core (Xie et al., 2006), etc. However,

extrinsic factors such as salts, pressure and substrate are also able to affect the enzyme thermostability. Indeed, substrate molecules have long been known to be able to improve the enzyme thermostability by stabilizing the active site (Vieille and Zeikus, 2001). However, to the best of our knowledge, the substrate stabilizing effect on family 11 xylanase was rarely reported and the stabilizing effect caused together by the substrate and xylanase amino-acid mutation was even less seen. It was obvious that a good understanding of the molecular basis for such effect may lead to new rules for rational design and engineering of thermophilic xylanases.

In this study, we report a single-point mutation (D57N) in the active center of a family 11 xylanase (Xyn-CDBFV) from *Neocallimastix patriciarum* resulting in that the substrate has a significant stabilizing effect on the mutant. The investigation of the molecular basis for such stabilizing effects will shed new lights on enzyme optimization processes.

---

*Corresponding authors. E-mail: honglu0211@yahoo.com Tel:/Fax: +86-21-65642505. (Hong Lu). E-mail: huangqiang@fudan.edu.cn. Tel: +86-21-55664934. (Qiang Huang).

Abbreviations: Xyn-CDBFV, a family 11 xylanase from *Neocallimastix patriciarum*; **CD**, circular dichroism; **PDB**, Protein Data Bank; **DNS**, 3, 5-dinitrosalicylic acid; **LB**, Luria-Bertani bacterial culture medium.

MATERIALS AND METHODS

Site-directed mutagenesis and cloning

Site-directed mutagenesis was carried out to produce Xyn-CDBFV-D57N mutant by two-step over-lapping PCR with Pfu polymerase

(Ho et al., 1989).

In the first-round PCR, CDBFV_sense_BamHI primer (5'-GGC*GGATCC*ATGCAAAGTTTCTGTAGTTCAGCTTCTCAC-3') and D57N_anti primer (5'-CATAAGTA*ATT*CCCAGCATTTTG-3') were used to amplify the first DNA fragment of about 200 bp with Xyn-CDBFV gene as the template, CDBFV_anti_NotI primer (5'-GCG*GCGGCCGC*ATCACCAATGTAAACCTTTGCGTA -3') and D57N_sense primer (5'-CAAAATGCTGGG*AAT*TACTTATGT -3') were used to amplify the second DNA fragment of about 500 bp with Xyn-CDBFV gene as the template. These two amplified fragments having overlapping ends were combined as the second-round PCR template using CDBFV_sense_BamHI primer and CDBFV_anti_NotI primer. These two primers were also used to amplify the wild type gene with Xyn-CDBFV gene as the template.

The PCR reaction mixture contained 41.5 µl of water , 5 µl of 10X Pfu reaction buffer, 1 µl of 40 mM dNTP mix (200 µM each final), 0.5 µl of each of flanking primers (250 ng/µl of each primer), 1 ng template DNA and 2.5 units of Pfu in a total volume of 50 µl. All amplifications were performed at 94°C for 30 s followed by 30 cycles at 94°C for 30 s, 58°C for 30 s and 72°C for 30 s. PCR products were separated by agarose gel electrophoresis and purified using BioDev PCR purification kit. Upon digestion with BamHI and NotI, the PCR products were ligated into the pET21a vector (Novagen, http://www.emdbiosciences.com/product/69740) digested with same enzymes. The ligation was catalyzed by T4 DNA ligase (TaKaRa, Dalian, China) at 16°C for 5 h, resulting in the expression plasmids of pET21a-Xyn-CDBFV and pET21a-Xyn-CDBFV-D57N. The full length of the gene was sequenced in Invitrogen (Shanghai, China).

Expression of recombinant proteins in *E. coli*

The constructed expression plasmids of pET21a-Xyn-CDBFV and pET21a-Xyn-CDBFV-D57N were transformed into *E. coli* strain BL21 (DE3). The BL21 (DE3) transformants were grown at 37°C in 100 ml LB media with 100 µg/ml ampicillin until the early exponential phase (OD$_{600}$ = 0.6 - 0.8). The protein expression was induced by 0.1 mM IPTG at 20°C for 15 h. Cells of 100 ml culture were harvested by centrifugation at 5000 rpm for 5 min and resuspended in 5 ml lysis buffer (50 mM Tris-HCl, 20 mM NaCl, pH 7.4) and then disrupted by ultrasonication. After centrifugation at 12000 rpm for 10 min, the supernatant was mixed with 1 ml Ni-NTA resin at 4°C for half an hour. After being washed with 5 ml washing buffer (50 mM Tris-HCl, 20 mM NaCl, 20 mM imidazole, pH 7.4), the Ni-NTA resin was eluted with 2 ml elution buffer (50 mM Tris-HCl, 20 mM NaCl, 250 mM imidazole, pH 7.4). The purity of proteins was judged by SDS-PAGE (5% acrylamide in stacking Gel, 15% acrylamide in resolving Gel) and Coomassie blue staining, according to the procedures described in Appendix 8 of Molecular Cloning: A Laboratory Manual (Third Edition).

Determination of catalytic parameters

The Michaelis-Menten steady-state parameters, K_m and k_{cat}, were determined using oat-spelt xylan (Fluka) as substrate. The parameters at various pHs were determined in 50 mM citric acid buffer (pH 3.5 - 5.5) and 50 mM Na$_2$HPO$_4$-NaH$_2$PO$_4$ buffer (pH 6.0 - 7.5) at 52°C and those at different temperatures were determined in 50 mM citric acid buffer (pH 5.0) at various temperatures. Typically, substrate concentrations were varied from 1 to 10 mg/ml. After 5 min incubation, the reduced sugar was determined by DNS method (Miller, 1959). Experimental rates measured at each given substrate concentration were plotted to the standard Michaelis-Menten expression. Values of k_{cat}/ K_m were determined from the slope of

Lineweaver-Burke plot (Joshi et al., 2001). Activation energy E_a was calculated from the k_{cat} values at those temperatures below the optimal temperature according to the Arrhenius equation

$$k_{cat} = Ae^{-\frac{E_a}{RT}},$$

where A is the Arrhenius constant related to steric effects and the molecular collision frequency, R is the gas constant (8.314 J mol^{-1} K^{-1}), T is the temperature (K).

Characterization of xylanase thermostability

The enzyme thermostability was characterized by the residual relative activity after incubation in 50 mM citric acid buffer (pH 5.0) at 72°C for 10 min in the absence or presence of the substrate (Vieille and Zeikus, 2001) and T_m which was calculated from circular dichroism (CD) spectra in 0.5 mM citric acid buffer (pH 5.0) (Ruller et al., 2008).

In the absence of the substrate, the enzyme was first incubated in 50 mM citric acid buffer (pH 5.0) at 72°C for 10 min, followed by enzyme activity assay in parallel with none-heat treated enzyme assay and then the relative residual activity was determined. While in the presence of the substrate, the substrate molecules were first mixed with enzyme in 50 mM citric acid buffer (pH 5.0) and then this mixture was split to four equal portions. The first portion (P1) was incubated at 72°C for 10 min; the second portion (P2) was also incubated at 72°C for 10 min and followed by 10 min incubation at 52°C; the third portion (P3) was incubated at 52°C for 10 min; the fourth portion (P4) was incubated at 52°C for 20 min. After incubation, the amounts of the reduced sugar of four portions (A1, A2, A3 and A4, respectively) were determined by DNS method. The thermostability in the presence of the substrate was represented by the ratio of the reduced sugar amount of P2 and P4 during the last 10 min incubation at 52°C (this ratio is $\frac{A2-A1}{A4-A3}$).

Circular dichroism (CD) spectra of the enzymes were measured using a JASCO 715 spectropolarimeter (JASCO, Tokyo, Japan) in 0.5 mM citric acid buffer (pH 5.0) in a 1 cm path-length quartz cuvette (Ruller et al., 2008). The temperatures of the sample were varied from 35 to 85°C at a rate of 1°C/min using a computer controlled Peltier heat exchange accessory, PTC-423S (JASCO). In order to eliminate baseline signal drift arising from the equipment, the spectropolarimeter and xenon lamp were turned on at least 30 min prior to the start of the experiments. Ellipticity values between 200 and 250 nm of the enzymes were continuously collected using an integration time of 5 min, from which the spectra of a buffer blank were subtracted. Ellipticity values at 220 nm were specifically extracted to determine the melting temperature (T_m) of transition from the native state to the unfolded state for the CD spectra that showed defined minima at 220 nm. After data smoothing, ΔH_{nu} (the enthalpy change between the native and unfolded proteins), ΔS_{nu} (the entropy change between the native and unfolded proteins) and T_m (the midpoint of the thermal unfolding transition determined by CD) for the CDBFV and mutant protein were estimated from the ellipticity changes measured during the thermal denaturation, as previously described (Sushma and Faizan, 2000).

Table 1. The catalytic and thermostability parameters of CDBFV and the D57N mutant*

Parameters	CDBFV	D57N
k_{cat} (S^{-1})	3895.47± 378.81	370.90 ± 13.39
K_m (mg/ml)	10.11 ± 1.40	1.82 ± 0.16
k_{cat} / K_m (ml/mg/S)	385.31 ± 15.99	203.67 ± 10.56
E_a (kJ/mol)	36.11	91.40
T_m (°C)	63.86	63.85
ΔH_{nu} (kJ/mol)	487.52	520.56
ΔS_{nu} (kJ/mol/K)	1.45	1.54

*The k_{cat} and K_m of Xyn-CDBFV and Xyn-CDBFV-D57N were determined at 72°C in 50 mM citric acid buffer (pH 5.0). E_a was determined from k_{cat} values at those temperatures below the optimal temperature according to the Arrhenius equation. T_m, midpoint of the thermal unfolding transition determined by CD. ΔH_{nu}, difference in the van't Hoff enthalpy between native and unfolded proteins. ΔS_{nu}, difference in the entropy between native and unfolded proteins.
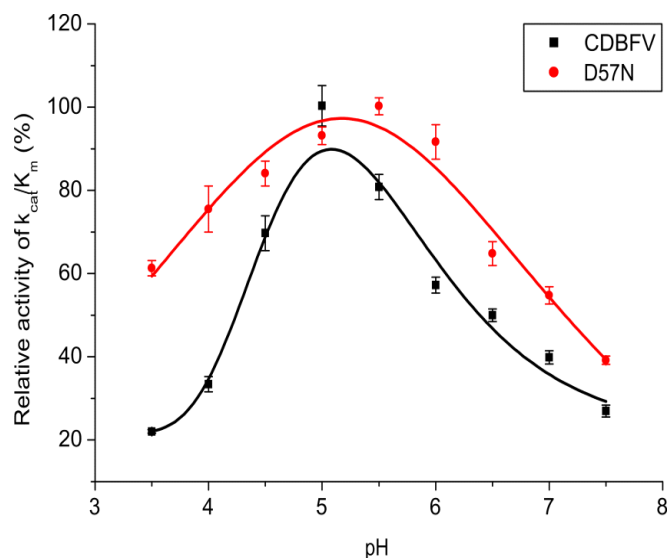

Figure 1. The k_{cat}/K_m relative values of Xyn-CDBFV and Xyn-CDBFV-D57N in 50 mM citric acid buffer (pH 3.5 - 5.5) and 50 mM Na$_2$HPO$_4$-NaH$_2$PO$_4$ (pH 6.0 - 7.5) at 52°C. Values shown are means of triplicate determinations. The data points were fitted with Lorentz function by OriginPro 8.5.

Molecular docking simulation

We used the program AutoDock 4.0 (http://autodock.scripps.edu/) to simulate the best binding modes of the substrate molecule to the family 11 xylanases. Three-dimensional structures of xylanases were downloaded from the Protein Data Bank (PDB) (http://www.pdb.org). The molecular structure of the substrate was generated and energetically optimized by the program suite Chem-Office. For each substrate, 30 low-energy binding conformations were generated and the substrate molecule which posses the same orientation as that in the crystallographic structure (PDB code: 1bcx) and has the lowest binding energy was selected for the binding site analysis. The predicted substrate-binding sites are those residues in which any atom is less than 3 Å away from the atoms of the substrate molecule.

RESULTS

Activity profiles of the wild type and the D57N mutant at various temperatures and pHs

In family 11 xylanases, the residue that has a hydrogen bond with the general acid/base catalyst at position 57 (CDBFV numbering) is an asparagine for the so-called 'alkaline' xylanases and an aspartic acid for the 'acidic' xylanases (Sapag et al., 2002). To engineer a more alkalophilic xylanase, we obtained the D57N mutant of a family 11 xylanase (CDBFV) from *Neocallimastix patriciarum*. As expected, the D57N mutant displays a higher optimal pH by 0.5 than the wild type (Figure 1). But the values of k_{cat} / K_m of the mutant are lower than the wild type. Both the acid limb and basic limb of the wild type show sharper than the mutant.

Then, we determined the temperature-dependent activity profiles of the wild type and the D57N mutant. The E_a of the mutant enzyme is about 3-fold greater than that of the wild type (Table 1), indicating the decreased reaction rate of the mutant. The k_{cat} / K_m values of the mutant are only 8 - 20% of the wild type below 72°C, while 30-60% above 72°C. But the optimal k_{cat} / K_m temperature of the mutant is 10 - 15°C higher than the wild type (Figure 2).

Activity assays of the *Pichia pastoris* secreted by wild type and D57N mutant enzymes were also performed under the same conditions. Similar results were seen (data not shown).

Thermostability of the wild type and the D57N mutant

In this study, the increased optimal temperature of the mutant will be attributed to the increased thermostability in the presence and (or) the absence of the substrate. We found that, in the absence of the substrate, after incubating at 72°C for 10 min in 50 mM citric acid buffer (pH 5.0), the relative residual activities of the two enzymes
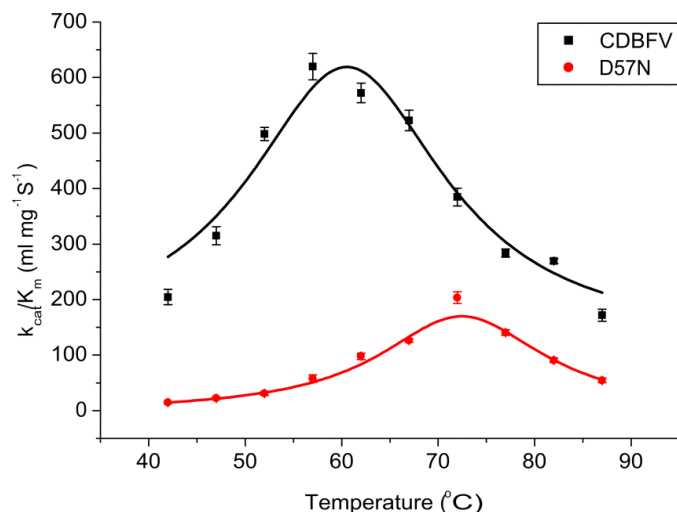
Figure 2. The k_{cat}/K_m values of Xyn-CDBFV and Xyn-CDBFV-D57N in 50 mM citric acid buffer (pH 5.0) at various temperatures from 42 to 87°C. Values shown are means of triplicate determinations. The data points were fitted with Lorentz function by OriginPro 8.5.
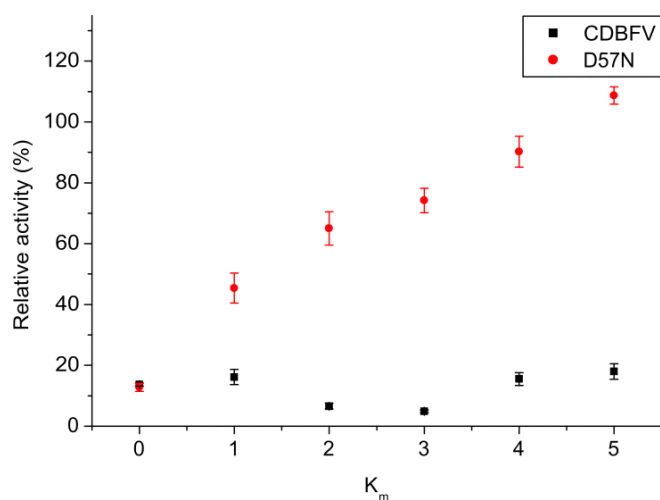

Figure 3. The relative residual activity values of Xyn-CDBFV and Xyn-CDBFV-D57N in 0, 1, 2, 3, 4 and 5 fold of K_m concentration of oat-spelt xylan after preheating at 72°C for 10 min in 50 mM citric acid buffer (pH 5.0). Values shown are means of triplicate determinations.

Figure 4. A. CD spectra (200 – 250 nm) of Xyn-CDBFV (solid line) and Xyn-CDBFV-D57N mutant (broken line) at 35°C in 0.5 mM citric acid buffer (pH 5.0). This indicates that the secondary structure of the D57N mutant is almost the same as that of the wild type. B. The ellipticity values of Xyn-CDBFV and Xyn-CDBFV-D57N in 0.5 mM citric acid buffer (pH 5.0) at 220 nm from 35 - 85°C.

differ little (Figure 3). This indicates that the thermo-stability of the two enzymes in the absence of the substrate is almost the same. This fact was further con-firmed by the similar T_m values of the two enzymes calcu-lated from CD spectra, as well as the similar ΔH_{nu} and ΔS_{nu} in the unfolding transition (Figure 4 and Table 1).

In the presence of the substrate, we investigated the substrate stabilizing effect on the two enzymes under the same substrate 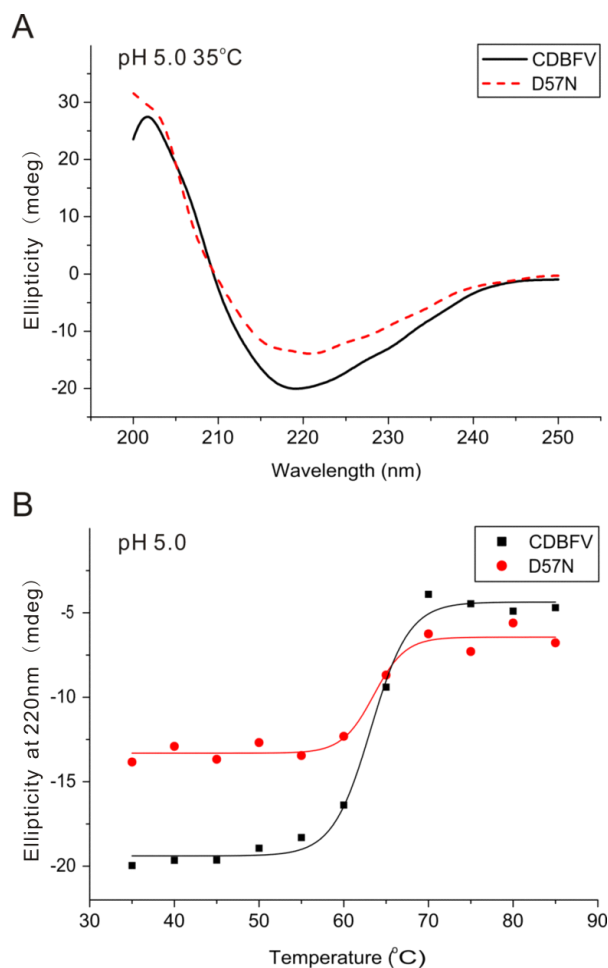binding affinity. As shown in Table 1, the K_m of the wild type and the mutant enzyme is 10.11 ± 1.40 mg/ml and 1.82 ± 0.16 mg/ml against xylan at 72°C, respectively (Table 1). We found that the relative residual activity of the wild type under 5-fold of K_m concentration of xylan is similar to that without xylan. However, the relative residual activity of the mutant increases with xylan concentration (Figure 3). Under 5-fold of K_m con-centration of xylan, the mutant enzyme almost retains full activity after incubation at 72°C for 10 min. This indicates that xylan has significant stabilizing effect on the D57N mutant.

Thus, the higher optimal temperature of the D57N mutant can be attributed to the substrate stabilizing effect. Since thermostable protein may tolerate extreme pH environ-ment (Vieille and Zeikus, 2001), this is why the acid limb and basic limb of the wild type show sharper than the mutant.

Table 2. The predicted substrate binding sites of some alkaline and acidic family 11 xylanases using AutoDock.

Site number	Alkaline xylanases						Acidic xylanases		
	1bcx	1igoB	1rex	1xnb	2c1f	2vgd	1bk1	1ukr	1xyn
57	+		+	+		+			
109	+	+		+	+		+	+	+
202			+	+	+	+			

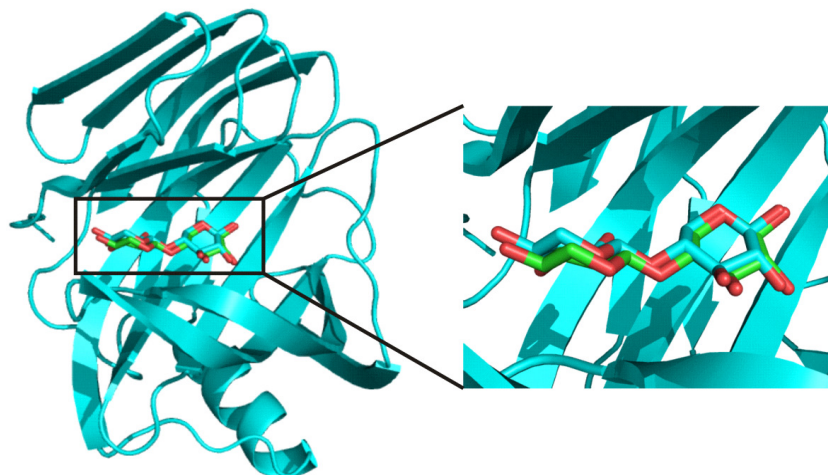The site numbers accords to the CDBFV site numbering.

Figure 5. The docking result of X-ray structure (PDB code: 1bcx) with xyloside. Green xyloside is the best-binding substrate predicted by AutoDock and cyan xyloside is the substrate molecule in glycosyl-enzyme structure (PDB code: 1bcx). RMSD between these two substrate molecules is 0.47 Å. The figure was generated with PyMol (http://pymol.sourceforge.net/).

Molecular docking of xylan molecule into family 11 xylanases

It is well known that the stacking of aromatic groups and hydrogen bonding are two major kinds of interactions between an enzyme and its substrate (Krengel and Dijkstra, 1996). Very likely, the substrate stabilizing effect on the D57N mutant may be attributed to the hydrogen bonds between N57 and the substrate molecule. To test this hypothesis, we employed a molecular docking approach to investigate the best binding mode of the substrate molecule with family 11 xylanases.

The widely used program AutoDock has been employed to perform molecular docking (Morris and Lim-Wilby, 2008; Morris et al., 2008). To test the reliability of this program for family 11 xylanases, we first carried out a test docking of xyloside with a family 11 xylanase, whose xyloside-enzyme intermediate crystal structure has been solved by Wakarchuk et al. (1994a) (PDB code: 1bcx) and this structure could be used as a comparison with the docking result. The position of the best-binding substrate molecule predicted by AutoDock was almost the same as that in the crystal structure (Figure 5), RMSD (root mean

square deviation) between these two substrate molecules is only 0.47 Å. Therefore, AutoDock is able to predict the binding mode of the substrate with family 11 xylanase reliably.

Since there is neither crystal nor NMR structure of Xyn-CDBFV, we performed molecular docking for the substrate molecule with available X-ray structures of alkaline and acidic xylanases in PDB. The PDB codes for these investigated xylanases are: 1bcx, 1igo (chain B), 1rex, 1xnb, 2c1f and 2vgd (alkaline xylanases), 1bk1, 1ukr and 1xyn (acidic xylanases). Because the active centers of family 11 xylanases can accommodate at least four xyloses (Kulkarni et al., 1999), we performed the docking simulations of these xylanases with xylotetraose. After investigating the putative binding sites of these xylanases, we found that N57, E202 (CDBFV numbering) are the additional substrate binding sites in the alkaline xylanases. However, there exists no such binding site in the acidic xylanases (Table 2). Thus, it appears that N57, E202 of the D57N mutant may be the additional substrate binding residues, which are able to mediate additional hydrogen bonding interaction with xylan and result in the mentioned stabilizing effect (Figure 6). On the other hand,
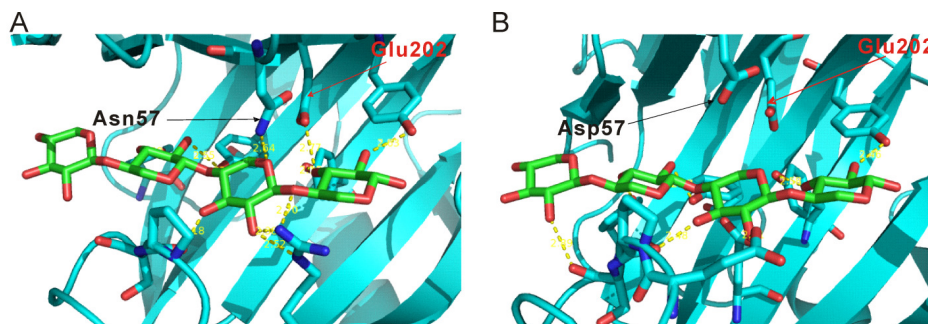
Figure 6. The putative substrate binding sites in an alkaline xylanase (A) and an acidic xylanase (B). The alkaline xylanase model is 2vgd (PDB code) and the acidic xylanase model is 1ukr (PDB code).

it has been found that there exists a strong hydrogen bond between D57 and E202 of the wild type enzyme in the glycosyl-enzyme intermediate (Joshi et al., 2000) and thus Asp57 and Glu202 function together as acid/base catalyst and may not play a role in binding substrate. This may weaken the interactions between the enzyme and the substrate.

DISCUSSION

To the best of our knowledge, here we reported for the first time that the interplay of an amino-acid mutation and the substrate could lead to further stabilizing effects on the mutant. This suggests that such substrate stabilizing effect may need to be considered in the engineering processes of protein thermostability.

Directed evolution has been proved to be a very powerful tool in protein engineering. A great deal of thermostable enzymes have been engineered by this approach (Dumon et al., 2008; Miyazaki et al., 2006; Ruller et al., 2008; Stephens et al., 2007). However, most of these mutant xylanases were engineered to be more thermostable than the wild type based on the intrinsic effects of the amino acid mutations on protein stability. The major reason is that the thermostability assays in the previous directed evolution were usually conducted without substrate. According to our results, it will be better to screen mutants with higher thermostability in the presence of the substrate. For example, we could determine the enzyme activities of a mutant at three or four different temperatures and the thermostability in the presence of the substrate will be represented by the relative activity values at the higher temperatures. Thus, the thermostable mutants screened by such a method will include not only the intrinsically thermostable mutants, but also the mutants which could be stabilized by the substrate. The latter mutants may be useful for us to reveal the substrate binding mechanism.

On the other hand, site-directed mutagenesis based on the rational design has long been used to improve the properties of protein (Jeong et al., 2007; Kimura et al.,

1992; Nikolova et al., 1998; Paes and O'donohue, 2006; Xiong et al., 2004). This method requires detailed knowledge about the protein to be engineered. Fortunately, many glycosyl-enzyme intermediate crystal structures of family 11 xylanases have been determined (Joshi et al., 2001; Sabini et al., 1999; Sidhu et al., 1999; Vardakou et al., 2008) and some computational tools such as Auto-Dock have been developed to identify the substrate binding sites. These will be very valuable for us to elucidate substrate binding mechanism, which is helpful in protein engineering with rational design in the presence of the substrate. The designed mutations may take place in the active site pocket. However, the mutations in the other regions of the protein have also been found to affect the thermostability in the presence of the substrate. For example, Turunen et al. carried out multiple Arg substitutions on the Ser/Thr surface of a family 11 xylanase from *Trichoderma reesei* and showed that although the mutant displayed the decreased thermostability in the absence of the substrate, the apparent optimal temperature of the mutant increases by ~5°C (Turunen et al., 2002). Very likely, the substrate further stabilizing effect on the mutant may lead to the increased thermostability.

Conclusion

We have shown that the D57N mutant of a family 11 xylanase (Xyn-CDBFV) from *N. patriciarum* could be further stabilized by the substrate, displaying a 10 - 15°C higher optimal temperature of activity than the wild type. Results of molecular docking indicated that the additional hydrogen bonding interactions between the substrate and residues N57, E202 of the mutant may account for such stabilizing effect. This provides new clues for screening thermophilic enzymes.

ACKNOWLEDGMENT

REFERENCES

Dumon C, Varvak A, Wall MA, Flint JE, Lewis RJ, Lakey JH, Morland C, Luginbuhl P, Healey S, Todaro T, DeSantis G, Sun M, Parra-Gessert L, Tan XQ, Weiner DP, Gilbert HJ (2008). Engineering hyperthermostability into a GH11 xylanase is mediated by subtle changes to protein structure. J. Biol. Chem. 283: 22557-22564.

Fenel F, Leisola M, Janis J, Turunen O (2004). A de novo designed N-terminal disulfide bridge stabilizes the *Trichoderma reesei* endo-1, 4-beta-xylanase II. J. Biotechnol. 108: 137-143.

Ho SN, Hunt HD, Horton RM, Pullen JK, Pease LR (1989). Site-directed mutagenesis by overlap extension using the polymerase chain reaction. Gene, 77: 51-59.

Jeong MY, Kim S, Yun CW, Choi YJ, Cho SG (2007). Engineering a de novo internal disulfide bridge to improve the thermal stability of xylanase from *Bacillus stearothermophilus* No. 236. J. Biotechnol. 127: 300-309.

Joshi MD, Sidhu G, Nielsen JE, Brayer GD, Withers SG, McIntosh LP (2001). Dissecting the electrostatic interactions and pH-dependent activity of a family 11 glycosidase. Biochemistry, 40: 10115-10139.

Joshi MD, Sidhu G, Pot I, Brayer GD, Withers SG, McIntosh LP (2000). Hydrogen bonding and catalysis: a novel explanation for how a single amino acid substitution can change the pH optimum of a glycosidase. J. Mol. Biol. 299: 255-279.

Kimura S, Kanaya S, Nakamura H (1992). Thermostabilization of *Escherichia coli* ribonuclease HI by replacing left-handed helical Lys95 with Gly or Asn. J. Biol. Chem. 267: 22014-22017.

Krengel U, Dijkstra BW (1996). Three-dimensional structure of Endo-1,4-beta-xylanase I from *Aspergillus niger*: molecular basis for its low pH optimum. J. Mol. Biol. 263: 70-78.

Kulkarni N, Shendye A, Rao M (1999). Molecular and biotechnological aspects of xylanases. FEMS Microbiol. Rev. 23: 411-456.

Miller GL (1959). Use of dinitrosalicylic acid reagent for determination of reducing sugar. Anal. Chem. 31: 426-428.

Miyazaki K, Takenouchi M, Kondo H, Noro N, Suzuki M, Tsuda S (2006). Thermal stabilization of *Bacillus subtilis* family-11 xylanase by directed evolution. J. Biol. Chem. 281: 10236-10242.

Morris GM, Huey R, Olson AJ (2008). Using AutoDock for ligand-receptor docking. Curr. Protoc. Bioinformatics Chapter 8; Unit 8; p. 14.

Morris GM, Lim-Wilby M (2008). Molecular docking. Methods Mol. Biol. 443: 365-382.

Nikolova PV, Henckel J, Lane DP, Fersht AR (1998). Semirational design of active tumor suppressor p53 DNA binding domain with enhanced stability. Proc. Natl. Acad. Sci. USA, 95: 14675-14680.

Paes G, O'Donohue MJ (2006). Engineering increased thermostability in the thermostable GH-11 xylanase from *Thermobacillus xylanilyticus*. J. Biotechnol. 125: 338-350.

Ruller R, Deliberto L, Ferreira TL, Ward RJ (2008). Thermostable variants of the recombinant xylanase A from *Bacillus subtilis* produced by directed evolution show reduced heat capacity changes. Proteins: Struct. Funct. Genet. 70: 1280-1293.

Sabini E, Sulzenbacher G, Dauter M, Dauter Z, Jorgensen PL, Schulein M, Dupont C, Davies GJ, Wilson KS (1999). Catalysis and specificity in enzymatic glycoside hydrolysis: a 2,5B conformation for the glycosyl-enzyme intermediate revealed by the structure of the *Bacillus agaradhaerens* family 11 xylanase. Chem. Biol. 6: 483-492.

Sapag A, Wouters J, Lambert C, de Ioannes P, Eyzaguirre J, Depiereux E (2002). The endoxylanases from family 11: computer analysis of protein sequences reveals important structural and phylogenetic relationships. J. Biotechnol. 95: 109-131.

Sidhu G, Withers SG, Nguyen NT, McIntosh LP, Ziser L, Brayer GD (1999). Sugar ring distortion in the glycosyl-enzyme intermediate of a family G/11 xylanase. Biochemistry, 38: 5346-5354.

Stephens DE, Rumbold K, Permaul K, Prior BA, Singh S (2007). Directed evolution of the thermostable xylanase from *Thermomyces lanuginosus*. J. Biotechnol. 127: 348-354.

Sushma Y, Faizan A (2000). A New Method for the Determination of Stability Parameters of Proteins from Their Heat-Induced Denaturation Curves. Anal. Biochem. 283: 207-213.

Turunen O, Vuorio M, Fenel F, Leisola M (2002). Engineering of multiple arginines into the Ser/Thr surface of *Trichoderma reesei* endo-1, 4-beta-xylanase II increases the thermotolerance and shifts the pH optimum towards alkaline pH. Protein Eng. 15: 141-145.

Vardakou M, Dumon C, Murray JW, Christakopoulos P, Weiner DP, Juge N, Lewis RJ, Gilbert HJ, Flint JE (2008). Understanding the structural basis for substrate and inhibitor recognition in eukaryotic GH11 xylanases. J. Mol. Biol. 375: 1293-1305.

Vieille C, Zeikus GJ (2001). Hyperthermophilic enzymes: sources, uses, and molecular mechanisms for thermostability. Microbiol. Mol. Biol. Rev. 65: 1-43.

Wakarchuk WW, Campbell RL, Sung WL, Davoodi J, Yaguchi M (1994a). Mutational and crystallographic analyses of the active site residues of the *Bacillus circulans* xylanase. Protein Sci. 3: 467-475.

Wakarchuk WW, Sung WL, Campbell RL, Cunningham A, Watson DC, Yaguchi M (1994b). Thermostabilization of the *Bacillus circulans* xylanase by the introduction of disulfide bonds. Protein Eng. 7: 1379-1386.

Xie H, Flint J, Vardakou M, Lakey JH, Lewis RJ, Gilbert HJ, Dumon C (2006). Probing the structural basis for the difference in thermostability displayed by family 10 xylanases. J. Mol. Biol. 360: 157-167.

Xiong H, Fenel F, Leisola M, Turunen O (2004). Engineering the thermostability of *Trichoderma reesei* endo-1, 4-beta-xylanase II by combination of disulphide bridges. Extremophiles, 8: 393-400.

Yang HM, Yao B, Meng K, Wang YR, Bai YG, Wu NF (2007). Introduction of a disulfide bridge enhances the thermostability of a *Streptomyces olivaceoviridis* xylanase mutant. J. Ind. Microbiol. Biotechnol. 34: 213-218.